

# PROGRESS TOWARD A LASER AMPLIFIER FOR OPTICAL STOCHASTIC COOLING\*

A.J. Dick, P. Piot<sup>1</sup>, Northern Illinois Center for Accelerator & Detector Development and Department of Physics, Northern Illinois University, DeKalb, IL, USA

M.B. Andorf, Cornell University, Ithaca, NY, USA

<sup>1</sup> also at Fermi National Accelerator Laboratory, Batavia, IL, USA

## Abstract

Optical Stochastic Cooling (OSC) is a method of beam cooling using optical frequencies which compresses the phase space of the beam by correcting the deviation of each particle's momentum. A particle bunch passing through an undulator produces radiation which is amplified and provides the corrective energy kick. In this project, we are testing a method of amplifying synchrotron radiation (SR) for the eventual use in OSC. The SR is amplified by passing through a highly-doped Chromium:Zinc Selenide (Cr:ZnSe) crystal which is pumped by a Thulium fiber laser. The SR will be produced by one of the bending magnets of the Advanced Photon Source. The first step is to detect and measure the power of SR using a photo-diode. The gain is then determined by measuring the radiation amplified after the single-pass through the crystal. This serves as a preliminary step to investigate the performance of the amplification of beam-induced radiation fields. The planned experiment is an important step towards achieving active OSC in a proof-of-principle demonstration in IOTA.

## INTRODUCTION

In the optical stochastic cooling (OSC) scheme, radiation produced by the particle bunch in the pickup undulator will pass through the crystal and be amplified [1, 2]. The amplified radiation is fed back into the kicker undulator and coupled back onto the same beam in such a way to produce a net corrective kick. The process is repeated multiple time in a storage ring leading to a gradual cooling of the beam. With proper lattice design, the cooling can be distributed over all 6-degrees of freedom in the phase space of the beam. The optical amplifier plays a crucial role in the cooling process and the selected amplification medium needs to provide the necessary gain but also provide amplification over a large bandwidth as the cooling time is inversely proportional to the optical-signal bandwidth. One potential lasing medium for the OSC proof-of-principle experiment at Fermilab's IOTA ring [3,4] is a thin Cr:ZnSe crystal pumped by a thulium fiber laser operating at 1908 nm [5]. The choice of the medium was dictated by its broadband in the mid-infrared which have a large overlap with the undulator radiation emitted from a 7-period undulator [6]; see Fig. 1.

\* This work is supported by U.S. Department of Energy under award No. DE-SC0013761 with Northern Illinois University and by the U.S. National Science Foundation under award PHY-1549132, the Center for Bright Beams.

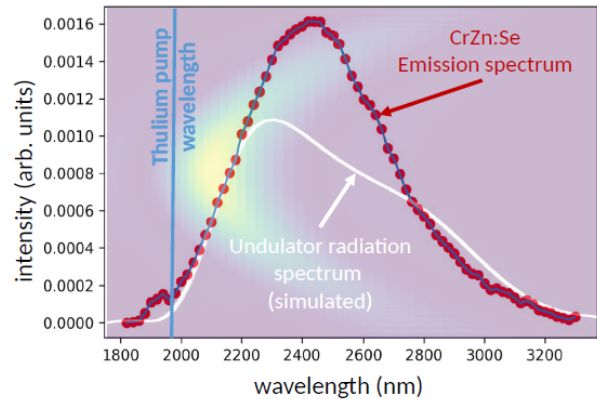


Figure 1: Measured CrZn:Te emission spectrum (red symbols) superimposed with the simulated on-axis undulator radiation (white trace). The false color image gives the angle (vertical axis)-wavelength intensity distribution associated with the undulator radiation; see Ref. [6] for the undulator radiation calculation.

To investigate the amplifier performances, we plan to use synchrotron radiation (SR) produced by one of the bending magnets at the Advanced Photon Source (APS). Specifically, our experiment will be installed in the 35BM beamline hutch. The amplifier setup comprises a Cr:ZnSe crystal which is pumped by a thulium fiber laser operating at 1908 nm. The experiment will guide the final design of the amplifier that will ultimately be incorporated in the active-OSC demonstration in IOTA. The topic discussed in this paper is a continuation of the work initiated in Ref. [7] and aimed at demonstrating amplification of electromagnetic radiation generated by an electron beam at the APS facility.

## AMPLIFICATION OF RADIATION

Amplification is produced in the crystal through stimulated emission caused by the broadband SR. The energy levels in the Cr:ZnSe crystal can be modeled as a four-level system. The pumping laser is responsible for populating the third excited state. From there, a radiation-free decay occurs to the second excited state. There are two main processes by which the second excited state falls back to the ground state. It may fall first to the first excited state then to ground or it may fall directly to ground. In the first case, emission from 2 to 1 can be stimulated by the signal SR. Then, like states 3 to 2, the decay from the first excited state to the ground state is radiation-free. In the second case, the wavelength

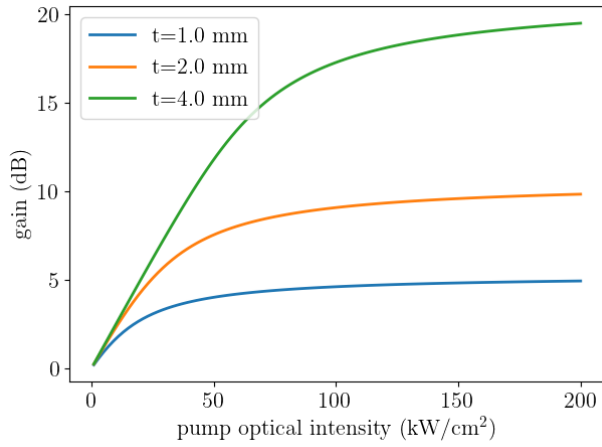


Figure 2: Single pass amplification gain of crystal as a function of average pumping intensity and for different crystal thicknesses of 1, 2, and 4 mm.

of the pump laser overlaps with the emission spectrum and may cause a decay from 2 directly to 0. These processes, of course, can occur spontaneously in the absence of a signal. The measurement of the spontaneous emission will verify the amplifier is working as expected before moving it to APS.

The gain through the amplifier can be derived from the rate relations [5] and is given by

$$G = \exp\left(\Delta I_p \frac{\sigma_s \tau_2}{h\nu_p}\right) \quad (1)$$

where  $\Delta I_p$  is the reduction in pumping intensity due to attenuation through the crystal,  $\sigma_s$  the emission cross section, and  $\nu_p$  the pump-laser frequency. The gain as function of pump-laser optical intensity for different crystal thickness appears in Fig. 2. The active OSC setup planned at IOTA requires a 1-mm-thick crystal to produce a 1.45 mm optical delay. This crystal pumped with an optical intensity of 125 kW/cm<sup>2</sup> produces a gain of 7 dB. However the proof-of-principle experiment will be performed with an off-the-shelf 4-mm thick crystal so to enable larger gains.

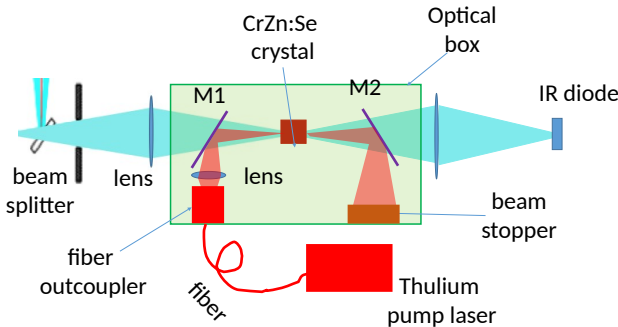


Figure 3: Single-pass amplifier configuration for the amplification of SR. M1 and M2 are dichroic mirrors.

A diagram of the amplifier to be used in the proof-of-principle experiment appears in Fig. 3. In brief, the SR radiation is focused on the crystal pumped by the Thulium laser which is injected/extracted from the interaction region with a pair of dichroic mirrors. The optical intensity downstream of the amplifier will be measured with a diode [HAMAMATSU (model C12492-210)] with an adequate spectral response in the wavelength range  $\lambda \in [1, 3.4] \mu\text{m}$ . Additionally, the spectrum measurement of the amplified radiation will be performed by a HORIBA scanning imaging spectrometer (model MICROHR).

## PUMP LASER

The Thulium-fiber laser was commissioned and its profile was measured using a knife-edge technique given the limited availability of two-dimensional detectors in the mid-IR region. The knife-edge plate was mounted to a THORLABS PT1-Z8 linear stage and the total power of the transmitted beam was measured using an OPHIR thermal power sensor. The method provides profile the cumulative integral associated with the laser profile  $S(r) = \int_{-\infty}^r I_0 e^{-2r'^2/w^2} dr'$  where  $r$  is the horizontal (or vertical) coordinates,  $I_0$  the on-axis optical intensity. Correspondingly the beam profile can be retrieved as  $I(r) = \frac{dS(r)}{dr}$  where the derivative is performed numerically on the discretized data set. An example of cumulative integral appears in Fig. 4. The setup can also be moved axially to measure the beam profile at various points along the optical axis  $\hat{z}$ . We generally observe that the beam pro-

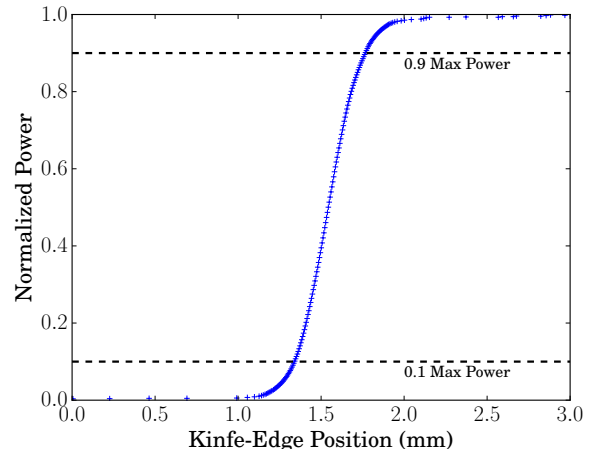


Figure 4: 10/90 method of determining beam profile width for power recorded from knife-edge profile

file is well described by a Gaussian distribution of the form  $I(r, z) = I_0(z)e^{-2r^2/w(z)^2}$  from which the beam-envelope radius can be measured. The radius of an ideal Gaussian beam evolves along the optical axis following [8]

$$w_r(z) = w_0 \sqrt{1 + \left(\frac{z}{z_r}\right)^2}$$

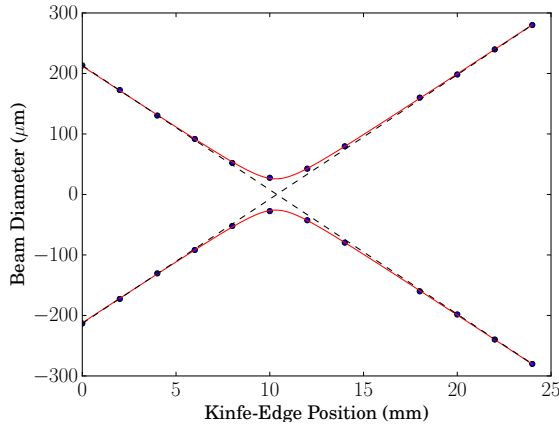


Figure 5: Thulium-laser beam envelope evolution measured downstream of a 10-mm-focal length lens. The blue dots correspond to data reported as  $\pm w(z_i)$  where  $z_i$  correspond to the position along the optical axis. The red traces are fit using Eq. 2.

which is the hyperbolic equation with asymptotic ( $z \gg z_r$ ) divergence given by  $\theta_{ideal} \approx w_0 \frac{z}{z_r} = \frac{\lambda}{\pi w_0}$ . The asymptotic divergence associated with a practical (real) beam is generally defined as [9]  $\theta_{real} = M^2 \frac{\lambda}{\pi w_0} = M^2 \theta_{ideal}$ . Consequently, the evolution along the optical axis can be written as

$$w_r(z) = w_0 \sqrt{1 + \left( M^2 \frac{z}{z_r} \right)^2} \quad (2)$$

where  $z_R \equiv \frac{\pi w_0^2}{\lambda}$  is the Rayleigh length,  $w_0$  the waist size,  $M^2$  the beam quality factor, and  $\lambda = 1908$  nm is the wavelength of the laser. The parameters  $w_0$ ,  $M$ , and  $z_R$  are inferred from a fit of the beam radii evolution measured along the optical axis.

The power distribution was measured for each point along the optical axis. The approximate Gaussian profile of the beam allows us to take advantage of certain properties of the Gaussian distribution. The locations at which the measured power is 10% and 90% of the maximum determine the beamwidth. Since the beam profile is nearly Gaussian we can relate the distance between these two points to the standard FWHM or  $1/e^2$  measurements of beam width because 80% of the beam is contained within  $1.281\sigma$ .

Since the thulium-laser beam is nearly collimated, we use a  $\text{CaF}_2$  lens with 10-mm focal length to focus the beam. The knife-edge plate was mounted on a motorized linear stage perpendicular to the optical axis. This stage was responsible for the individual beam profile measurements. Another linear stage moved the plate along the optical axis  $\hat{z}$ . Figure 4 summarizes the measured evolution of the beam size along the optical axis.

The measured beam radii were fitted to Eq. 2 to determine the waist size to be  $w_0 = 26.37 \mu\text{m}$  and  $M^2 \approx 1.012$ . This

can be seen in Figure 5. The value of  $M^2$  approaching unity is indicative of the high beam quality. It should be noted that the measured waist size corresponds to an optical intensity of about  $I_0 = P/(\pi w_0^2) \approx 1.9 \text{ MW/cm}^2$  (given the operating power of 40W). The latter value is well above the targeted  $125 \text{ kW/cm}^2$ ; see Fig. 2. In practice, we will use a longer focal lens to increase the waist size and reduce the Rayleigh range within the amplifier crystal.

## FUTURE PLANS

In the next few weeks, we plan to assemble the laser amplifier shown in Fig. 3 and characterize the properties of the spontaneous emission from the available crystal. In parallel, the knife-edge setup will be moved to the BM35 beamline at APS to measure the beam parameter associated with the SR beam and devise the proper optical configuration necessary to focus the SR beam on the amplifier crystal. It is anticipated that the SR amplification experiment will be performed by end of CY19.

## REFERENCES

- [1] A.A. Mikhailichenko and M.S. Zolotarev, "Optical Stochastic Cooling," *Phys. Rev. Lett.*, vol. 71, p. 4146, 1993.
- [2] M.S. Zolotarev and A.A. Zholents, "Transit-time method of optical stochastic cooling," *Phys. Rev. E*, vol. 50, p. 3087, 1994.
- [3] V. A. Lebedev and A. L. Romanov, "Optical Stochastic Cooling at IOTA ring", in *Proc. 10th Workshop on Beam Cooling and Related Topics (COOL'15)*, Newport News, VA, USA, Sep.-Oct. 2015, paper WEWAUD03, pp. 123–127.
- [4] J. Jarvis, S. Chattopadhyay, V. Lebedev, H. Piekarczyk, P. Piot, A. L. Romanov, J. Ruan, "Optical stochastic cooling at Fermilab's Integrable Optics Test Accelerator," presented at the North American Particle Accelerator Conf. (NAPAC'19), Lansing, MI, USA, Aug.-Sep. 2019, paper TUPLM21, this conference.
- [5] M.B. Andorf "Light Transport and Amplification for a Proof-of-Principle Experiment of Optical Stochastic Cooling," 2018, Northern Illinois University. doi:10.2172/1462087
- [6] M. B. Andorf, V. A. Lebedev, J. Jarvis, and P. Piot "Computation and Numerical Simulation of Focused Undulator Radiation for Optical Stochastic Cooling," *Phys. Rev. Accel. Beams*, vol. 21, no. 10, p. 100702, 2018.
- [7] M.B. Andorf and P. Piot, "Planned Detection and Amplification of Infrared Synchrotron Radiation for Electron-Beam Diagnostics and Manipulations," in *Proc. IPAC'18*, Vancouver, BC, Canada, Apr. 4, pp. 3358–3360. doi:10.18429/JACoW-IPAC2018-THPAK058
- [8] J. Peatross and M. Ware, *Physics of Light and Optics*, 2015 edition, available at [optics.byu.edu](http://optics.byu.edu)
- [9] ISO 11146-2:2005, Lasers and Laser-Related Equipment – Test Methods for Laser Beam Widths, Divergence Angles and Beam Propagation Ratios <https://www.iso.org/standard/33626.html>